Received: 9 December 2021 | Revised: 28 March 2022 | Accepted: 3 April 2022

DOI: 10.1111/cas.15366

ORIGINAL ARTICLE

Cancer Science WILEY

Long noncoding RNA *lnc-H2AFV-1* promotes cell growth by regulating aberrant m6A RNA modification in head and neck squamous cell carcinoma

Xi Chen[1] | Yunxia Liu[1,2] | Dongyuan Sun[1] | Rongqi Sun[1] | Xiaoxiao Wang[1,2] | Minmin Li[1] | Ning Song[1] | Jicheng Ying[1] | Tao Guo[3] | Yingying Jiang[1,2,4]

[1]School of Stomatology, Weifang Medical University, Weifang, China

[2]Department of Dentistry, Affiliated Hospital of Weifang Medical University, Weifang, China

[3]Department of Pathophysiology, School of Basic Medical Sciences, Weifang Medical University, Weifang, China

[4]Department of Oral and Maxillofacial-Head & Neck Oncology, Shanghai Ninth People's Hospital, Shanghai Jiao Tong University School of Medicine, Shanghai, China

Correspondence
Yingying Jiang, Department of Preventive Dentistry, School of Stomatology, Weifang Medical University, 7166, Bao Tong West Street, Weifang 261053, China.
Email: jiangyy@wfmc.edu.cn

Tao Guo, Department of Pathophysiology, School of Basic Medical Sciences, Weifang Medical University, 7166, Bao Tong West Street, Weifang 261053, China.
Email: guotao@wfmc.edu.cn

Funding information
This study was supported by grants from the National Natural Science Foundation of China (82103008), Shandong Provincial Natural Science Foundation (ZR2020MH192, ZR2020MH188), Shandong Provincial College Students Innovation and Entrepreneurship Training Program (S202110438038, S202110438022), and College students Innovation and Entrepreneurship Training Program of Weifang Medical University (X2021332). This study was also supported by the National Facility for Translational Medicine (Shanghai) (TMSF-2021-2-003), and 2021 Youth Innovation Talent Introduction and Education Program of Shandong Province Universities (Yingying Jiang).

Abstract

Head and neck squamous cell carcinoma (HNSCC) is the most common malignant tumor in the oral and maxillofacial regions, and long noncoding RNAs (lncRNAs) play crucial roles in the occurrence and progression of HNSCC. The lncRNA *lnc-H2AFV-1* was found to be upregulated in HNSCC tissues; however, the function of *lnc-H2AFV-1* in regulating HNSCC proliferation and the potential molecular mechanism is unclear. The present study evaluated the expression of *lnc-H2AFV-1* in HNSCC tissues using quantitative real-time PCR (qPCR) and associated abundant *lnc-H2AFV-1* expression with tumor size. Functionally, *lnc-H2AFV-1* significantly promoted the proliferation of HNSCC cells in vitro and in vivo. Quantified N6-methyladenosine (m6A) RNA methylation and dot blot assays revealed that total m6A methylation in HNSCC cells was accompanied by *lnc-H2AFV-1* expression. Western blotting showed that the expression of methyltransferase-like (METTL) 3 and METTL14 was consistent with that of *lnc-H2AFV-1*, whereas the expression of demethylase fat mass and obesity-associated (FTO) was contrary to that of *lnc-H2AFV-1*. Methylated RNA immunoprecipitation sequencing (MeRIP-seq) and MeRIP-qPCR revealed that *lnc-H2AFV-1* overexpression led to the elevated expression and maximal m6A methylation of intraflagellar transport (IFT) 80 in HNSCC. In addition, METTL3/14 knockdown decreased *IFT80* expression. Thus, our findings suggested that *lnc-H2AFV-1* might be a biomarker that alters m6A modification by regulating the m6A methylases METTL3/14 and FTO and then mediating the downstream target *IFT80* to promote HNSCC progression.

KEYWORDS
cell growth, head and neck squamous cell carcinoma, lnc-H2AFV-1, long noncoding RNA, N6-methyladenosine

1 | INTRODUCTION

Head and neck squamous cell carcinoma (HNSCC) is one of the most prevalent malignant tumors of the oral and maxillofacial regions. Over 600,000 new HNSCCs are diagnosed annually worldwide.[1–3] Although technological advances in surgery, radiotherapy and chemotherapy have improved local control of HNSCC, the 5-year survival rate remains low.[4] Therefore, clarifying the genetic and epigenetic molecular alterations associated with HNSCC is of great significance in improving the diagnosis, appropriate treatment, and prognosis of patients with HNSCC.

Long non-coding RNA (lncRNAs) are products of RNA transcription comprising >200 nucleotides without protein-coding potential. LncRNAs are important regulatory factors in cell biology and participate in DNA replication, RNA transcription, protein translation, and cell development.[5] Many investigators, including the authors, have found that lncRNAs are closely associated with the occurrence and development of HNSCC.[6–8]

Current interest is increasingly directed towards reversible post-transcriptional modifications of RNA. Among these, the N6-methyadenosine (m6A) modification is the most abundant and conserved type of mammalian mRNA methylation.[9] This modification has been implicated in diverse biological processes, including tumorigenesis. Several molecules, such as methyltransferase-like (METTL) 3, METTL14, and demethylase fat mass and obesity-associated (FTO), actively participate in human cancers.[10–13] Therefore, the function of the m6A modification in the tumor diagnosis and prognosis of HNSCC requires further investigation, as it might provide a novel therapeutic target.

Regulators of m6A play roles in predicting the prognosis of patients with HNSCC.[14,15] Furthermore, m6A regulates the expression and function of lncRNAs.[16] However, the regulatory effect of lncRNAs on m6A has not yet been recognized. Here, we found that the lncRNA *lnc-H2AFV-1* was upregulated in HNSCC tissues and cell lines. We aimed to identify the function of *lnc-H2AFV-1* in HNSCC cells and to reveal the mechanism of *lnc-H2AFV-1* regulating m6A methylation. We further explored the downstream targets of *lnc-H2AFV-1* that enhance HNSCC progression. This might offer novel targets and directions for HNSCC prevention and treatment.

2 | MATERIALS AND METHODS

2.1 | Specimens

The specimens and clinicopathological information about the patients with HNSCC are described in our previous reports.[7,17]

2.2 | Cell lines and cell culture

We used the HNSCC cell lines HN4, HN6, HN30, SCC-4, SCC-9, SCC-25, and CAL-27, from the described sources,[7] and Table S1 lists the Research Resource Identifiers (RRIDs). Normal oral epithelial cells were cultured in keratinocyte serum-free medium (KSF; Gibco-BRL) with 0.2 ng/mL recombinant epidermal growth factor (rEGF; Invitrogen).

2.3 | Total RNA extraction and qPCR

Total RNA was extracted using the TRIzol Reagent and reverse transcribed using the PrimeScript RT Reagent Kit (Takara Bio) to generate cDNA. All qPCRs included the primers (Sangon Biotech) listed in Table S2 and proceeded using the TB Green Premix Ex Taq Reagent Kit (Takara) as described[8] and an ABI 7500 Fast Real-Time PCR System (Life Technologies).

2.4 | Western blotting

Proteins of interest were assessed using western blotting as described.[8,18] The primary antibodies comprised anti-METTL3 (Cat# 15073–1-AP; 1:1,000), anti-METTL14 (Cat# 26158–1-AP, 1:500), anti-FTO (Cat# 27226–1-AP, 1:1,000), and anti-beta actin (Cat# 20536–1-AP, 1:1,000) (all from Proteintech Group), and HRP-labeled anti-rabbit antibody (1:10,000, Cell Signaling Technology) was the secondary antibody. Signals were visualized using an ECLUltra (New Cell and Molecular Biotech).

2.5 | Smart silencer/antisense oligonucleotide, siRNA, or plasmid transfection

The smart silencer/antisense oligonucleotides (ASOs) and siRNAs were designed and synthesized (Guangzhou RiboBio), and Table S3 shows their sequences. The plasmids were constructed by HanYin Biotechnology. Cells were transfected using Lipofectamine 3000 (Invitrogen), as described by the manufacturer.

2.6 | Lentiviral transduction and screening stable strains

lnc-H2AFV-1 lentiviral vectors (LV-lnc-H2AFV-1) were constructed (HanYin Biotechnology). Lentiviral transduction was performed according to the manufacturer's instructions. After 72 h of transfection, the cells were cultured with a final concentration of 10 μg/mL puromycin, and the stably stained cells were screened after two to three passages.

2.7 | CCK-8

Cells (1×10^3/well) transfected with smart silencer/siRNA/plasmid for 24 h or stably transduced with lentivirus were seeded into 96-well plates in triplicate. The cells were incubated at 37°C for 2 h with 10 μL of CCK-8 reagent (Dojindo), and optical density was measured

at 450 nm using a Multiskan Go Microplate Reader (Thermo Fisher Scientific) every day for 5 days.

2.8 | Colony formation assays

Cells (1×10^3/well) transfected with smart silencer/siRNA/plasmid for 24 h or stably transduced with lentivirus were seeded into six-well plates and cultured for 10–14 days. Colonies were fixed with 4% paraformaldehyde (Beyotime), stained with crystal violet (Beyotime), and counted manually using an anatomical microscope (Leica S8APO Stereo Microscope, Leica Microsystems).

2.9 | 5-ethynyl-20-deoxyuridine assays

Cell proliferation was assayed using a 5-ethynyl-2′-deoxyuridine (EdU) kit (RiboBio), as described by the manufacturer. Cells (1×10^6 cells/well) seeded into confocal plates were cultured in 50 μM EdU buffer for 2 h at 37°C, fixed with 4% formaldehyde for 0.5 h, and permeabilized with 0.1% Triton X-100 (Sigma-Aldrich) for 20 min. Thereafter, EdU solution was added to the medium and the cells stained with Hoechst were assessed using a fluorescence microscope (Carl Zeiss Meditec AG).

2.10 | Isolation of nuclear and cytoplasmic RNA

Nuclear, cytoplasmic, and total RNA were isolated using a PARIS Kit (Thermo Fisher Scientific), as described by the manufacturer. After purification of RNA from nuclear/cytoplasmic fractions and then removal of trace genomic DNA using DNase I (Beyotime), the nuclear and cytoplasmic RNA was reverse-transcribed and amplified by qPCR, as described above.[7,8,18] The endogenous controls were *MALAT1*, *NEAT1*, *TUG1*, and *U6* for the nucleus and *BIRC5* and β-actin for the cytoplasm.

2.11 | FISH

Fluorescence-labeled probes for *lnc-H2AFV-1* and *U6* RNA were designed and synthesized, and FISH proceeded using a Ribo Fluorescent In Situ Hybridization Kit (RiboBio). Images were acquired using a TCS SP8 laser scanning confocal microscope (Leica).

2.12 | Xenograft formation and in vivo metastasis assay

All animal experiments involving BALB/c nude mice (4 weeks old) (Medical Laboratory Animal Center of Weifang Medical University, Weifang, China) complied with appropriate ethical standards and national guidelines. To determine whether *lnc-H2AFV-1* overexpression could enhance tumorigenicity in vivo, 1×10^6 HN6 cells stably transduced with LV-lnc-H2AFV-1 or LV-NC were subcutaneously injected into the right and left flanks of six mice, respectively. We assessed the ability of *lnc-H2AFV-1* knockdown to inhibit tumorigenesis in vivo, by establishing a xenograft tumor mouse model using cholesterol-conjugated *lnc-H2AFV-1* ASO (ASO-lnc-H2AFV-1) for in vivo ASO delivery (sequences shown in Table S3). The cell lines and operating methods used in animal experiments have been applied repeatedly in previous studies, and the procedures and precautions are detailed elsewhere.[7,8] The mice were killed; then tumor samples were collected, weighed, and embedded in paraffin for H&E staining and immunohistochemistry (IHC).

2.13 | Immunohistochemistry

Sections were immunohistochemically stained as described.[8] Consecutively, 4-μm-thick sections were analyzed using primary antibodies against Ki-67 (Cat# ab833, 1:50, Abcam) and biotin-conjugated goat anti-rabbit polyclonal antibody (1:50; ZSGB-BIO) as the secondary antibody. Images were captured using a light microscope (Olympus).

2.14 | Dot blot assay of m6A

Total RNA isolated as described above was dissolved in three volumes of incubation buffer and denatured at 65°C for 5 min. Samples (500 and 250 ng) in ice-cold 20× SSC buffer (Sigma-Aldrich) were loaded onto a nylon-N+ membrane (Beyotime). The membrane was UV-crosslinked for 5 min and stained with 0.02% methylene blue (Sangon Biotech) to determine the total content of input RNA. The membrane was incubated with specific m6A antibody (1:1000; CST) overnight at 4°C. Dot blots were incubated with HRP-conjugated anti-mouse IgG for 1 h before visualization using an imaging system (Bio-Rad Laboratories).

2.15 | Quantitation of m6A RNA methylation

Levels of m6A in total RNA were determined using an EpiQuik m6A RNA Methylation Quantification Kit (Colorimetric) (Epigentek), as described by the manufacturer. Briefly, total RNA (200 ng) and m6A standard were bound to 96-well plates, which was captured and detected with antibodies. Enhancer and color-developing solutions were added; then m6A levels were quantified colorimetrically at a wavelength of 450 nm, and calculations were based on a standard curve.

2.16 | Sequencing m6A MeRIP and data analyses

m6A MeRIP-sequencing and data analyses were supported by OE Biotechnology. For RNA fragmentation and m6A MeRIP, the protocols from previously published literature were followed.[19] With respect to the data analysis, both m6A-IP and input reads were aligned to the human genome (UCSC hg19) using HISAT2 v.2.1.0.[20] m6A

peak calling and differential analysis of m6A methylation were performed using MeTDiff v.1.1.0.[21] MEME-ChIP v.5.0.5[22] was used to search for the enriched motif in the m6A peak region. m6A peak distribution in the screened genes was visualized using the Integrative Genomics Viewer (IGV).[23] GO enrichment and KEGG pathway enrichment analysis of DEGs were performed using R the clusterProfiler package. $P < 0.05$ and |log2(foldchange)|>0.58 was set as the threshold for a significant m6A peak and significant differential expression.

2.17 | MeRIP-quantitative real-time PCR

MeRIP assay was performed using a riboMeRIP m6A Transcriptome Profiling Kit (RiboBio) to determine the m6A modifications of individual transcripts. Briefly, total RNA was fragmented, and 10% was saved as the input. The fragmented RNA was incubated with anti-m6A antibody and normal rabbit IgG conjugated to magnetic beads A/G for 2 h at 4°C. Bound RNA was eluted from the beads with elution buffer for 1 h at 4°C and purified using an RNA Purification Kit (TIANGEN). The input and m6A-enriched RNAs were reverse-transcribed with random hexamers, and enrichment was determined by qPCR.

2.18 | Statistical analysis

All data were statistically analyzed using the Statistical Package for Social Science software v.16.0 (SPSS 16.0; SPSS) and GraphPad Prism 7.0 (GraphPad Software). Data are shown as means ± standard deviation (SD) and are representative of at least three independent experiments. Differences between groups were analyzed using one-way analysis of variance (ANOVA) or *t*-tests (two groups). Correlations between *lnc-H2AFV-1* levels and clinical features were analyzed using Mann–Whitney *U*-tests. Statistical significance was set at $P < 0.05$.

3 | RESULTS

3.1 | Upregulation of *lnc-H2AFV-1* expression in head and neck squamous cell carcinoma tissues correlated with tumor size

By querying the LNCipedia (https://lncipedia.org)[24] and the Ensembl (http://www.ensembl.org)[25] databases, it was determined that *lnc-H2AFV-1* (also known as ENSG00000228596 and AC013436.6) is located on human chromosome 7:44785050–44787340 and is transcribed as a 422-nt transcript (Figure S1A, B). ENST00000425077 (also known as lnc-H2AFV-1:1) has two exons but no protein-coding functions (http://www.ensembl.org/Homo_sapiens/Transcript/Summary?db=core;g=ENSG00000228596;r=7:44785050-44787340;t=ENST00000425077, Figure S1C). The expression profile of *lnc-H2AFV-1* in HNSCC from The Cancer Genome Atlas (TCGA) was analyzed using The Encyclopedia of RNA Interactomes (ENCORI, https://starbase.sysu.edu.cn)[26] and Gene Expression Profiling Interactive Analysis (GEPIA, http://gepia.cancer-pku.cn)[27] database, and the expression of *lnc-H2AFV-1* was upregulated in HNSCC tissues (Figure 1A, Figure S1D). *lnc-H2AFV-1* was correlated with many types of cancer using the LncRNADisease 2.0 (http://www.rnanut.net/lncrnadisease/)[28] database (Figure 1B, Figure S1E). We detected the expression of *lnc-H2AFV-1* in 68 pairs of HNSCC tissues and adjacent normal tissues from the *Sharing platform for the tissue sample and bioinformatics database of oral maxillofacial tumor* (http://mdl.shsmu.edu.cn/OMNDB/page/home/home_en.jsp)[7,17]. The results revealed significantly higher *lnc-H2AFV-1* expression in HNSCC tissues than in the adjacent tissues (Figure 1C,D). By analyzing the correlation between *lnc-H2AFV-1* expression and clinicopathological features of these 68 HNSCC tissues, we found that the expression of *lnc-H2AFV-1* was positively associated with tumor size; that is, the expression of *lnc-H2AFV-1* in HNSCC tissues >4 cm was higher than in HNSCC tissues ≤4cm (Figure 1E, Table 1). However, other clinicopathological features, such as sex, age, smoking, alcohol, TNM stage, tumor site, and lymph node metastasis, were not significantly associated with *lnc-H2AFV-1* expression (Table 1). Compared with its expression in primary normal oral epithelial cells, *lnc-H2AFV-1* expression was upregulated in seven HNSCC cell lines and was the most and least abundant in CAL-27 and HN6 cells, respectively (Figure 1F).

3.2 | Proliferation of head and neck squamous cell carcinoma cells in vitro was promoted by *lnc-H2AFV-1*

We investigated the functional role of *lnc-H2AFV-1* in HNSCC by transfecting CAL-27 and SCC-9 cells with the smart silencer specifically targeting *lnc-H2AFV-1* (SS-lnc-H2AFV-1) to knock down the relative expression of *lnc-H2AFV-1* (Figure 2A). Knockdown of *lnc-H2AFV-1* significantly suppressed cell proliferation according to the findings of CCK-8, colony formation, and EdU assays (Figure 2B-D).

To better characterize the function of *lnc-H2AFV-1* in HNSCC cells, *lnc-H2AFV-1* was overexpressed in HN6 and SCC-9 cells through transfection with *lnc-H2AFV-1* vector (Figure 2E, Figure S2). The results of CCK-8, colony formation, and EdU assays showed that *lnc-H2AFV-1* overexpression promoted cell proliferation in HN6 and SCC-9 cells (Figure 2F–H). Overall, these findings indicated that *lnc-H2AFV-1* profoundly impacted HNSCC cell proliferation.

3.3 | *Lnc-H2AFV-1* was mostly localized in nuclei of head and neck squamous cell carcinoma cells

We determined the subcellular localization of *lnc-H2AFV-1* in HNSCC cells using cytoplasmic/nuclear fractionation (Figure 3A)

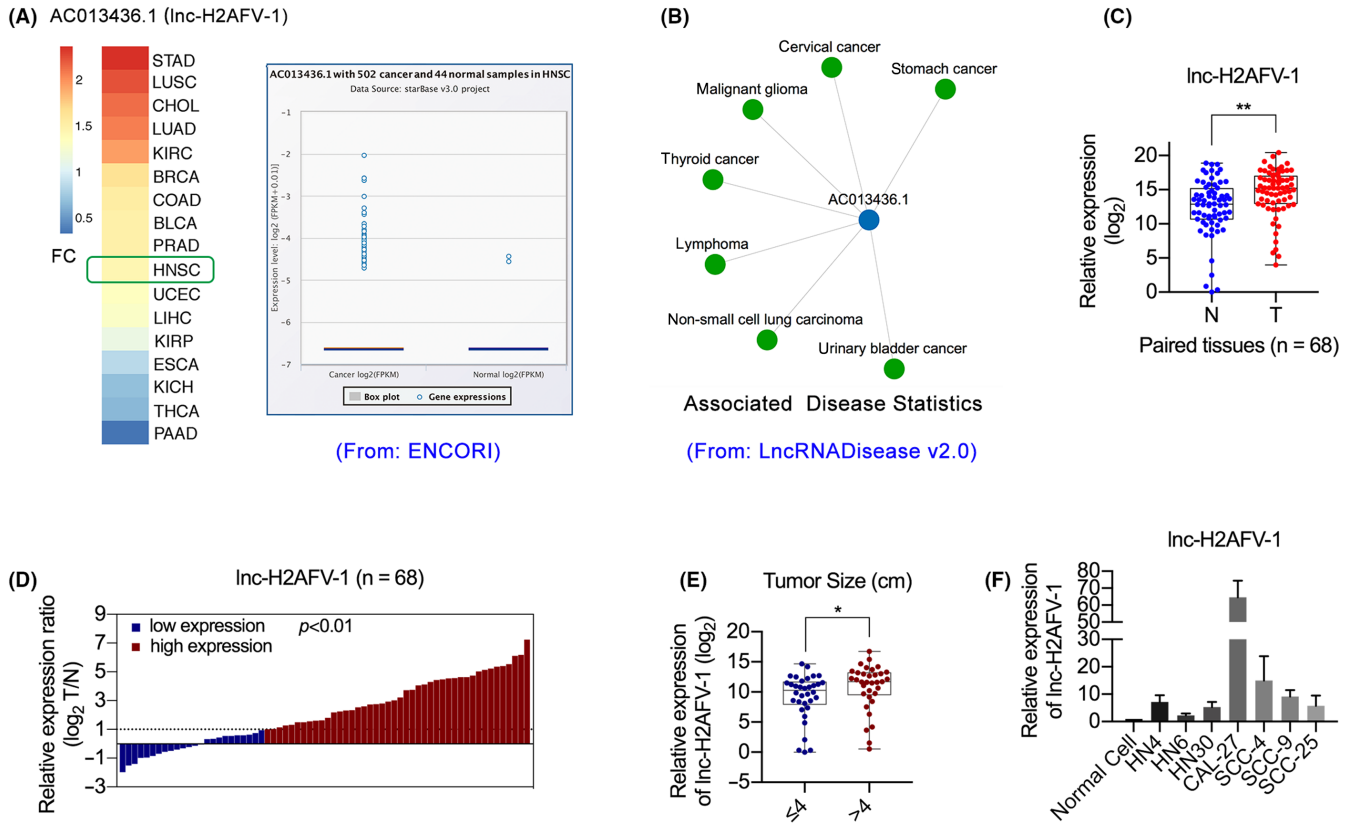

FIGURE 1 Expression of *lnc-H2AFV-1* is upregulated in head and neck squamous cell carcinoma (HNSCC) tissues. (A) Expression of *lnc-H2AFV-1* (AC013436.1) in 17 cancer datasets, including the HNSC dataset (502 cancer *vs* 44 normal samples) from the TCGA determined in the ENCORI database. (B) Diseases associated with *lnc-H2AFV-1* predicted by LncRNADisease database. (C) Relative expression of *lnc-H2AFV-1* in HNSCC (T) and adjacent normal (N) tissues determined using quantitative real-time PCR (qPCR). (D) Classification of *lnc-H2AFV-1* expression into groups according to expression ratios of HNSCC tumors to adjacent normal (T/N) tissues. (E) The association between *lnc-H2AFV-1* and tumor size determined in patients with HNSCCs. (F) Relative expression of *lnc-H2AFV-1* in seven HNSCC cell lines and normal oral epithelial cells, as detected using qPCR. $^{*}P < 0.05$, $^{**}P < 0.01$

TABLE 1 Relationship between lnc-H2AFV-1 expression and clinicopathologic features ($n = 68$)

Characteristics	Patients		lnc-H2AFV-1 ΔCt[a]		
	Number	%	Mean ± SD	Non-parametric test value	*P*value
Age (years)					
≥60	42	61.76	4.226 ± 3.968	Z = 0.404	0.686
<60	26	38.24	4.336 ± 3.795		
Gender					
Male	46	67.65	4.217 ± 3.726	Z = 0.170	0.865
Female	22	32.35	4.374 ± 4.257		
Smoking history					
Non-smoker	42	61.76	3.767 ± 3.463	Z = 0.871	0.384
Smoker	26	38.24	5.078 ± 4.411		
Alcohol history					
Nondrinker	46	67.65	3.859 ± 3.724	Z = 1.062	0.288
Drinker	22	32.35	5.124 ± 4.128		
Tumor size (cm)					
≤4	34	50.00	5.074 ± 3.841	Z = 2.318	0.020*
>4	34	50.00	3.462 ± 3.793		

(Continued)

TABLE 1 (Continued)

Characteristics	Patients		lnc-H2AFV-1 ΔCt[a]		
	Number	%	Mean ± SD	Non-parametric test value	*P*value
Lymph node metastasis					
pN0	31	45.59	4.203 ± 3.657	Z = 0.388	0.698
pN1 to pN3	37	54.41	4.323 ± 4.097		
TNM stage					
I	6	8.82	5.703 ± 3.565	H = 4.379	0.223
II	9	13.24	5.435 ± 3.977		
III	11	16.18	4.838 ± 5.055		
IV	42	61.76	3.664 ± 3.550		
Pathological differentiation					
Well	46	67.65	4.404 ± 4.150	Z = 0.039	0.969
Moderately/poorly	22	32.35	3.985 ± 3.295		
Disease Site					
Tongue	27	39.71	5.350 ± 4.735	H = 5.902	0.207
Gingival	20	29.41	3.486 ± 3.860		
Cheek	12	17.65	3.310 ± 1.489		
Floor of mouth	3	4.41	8.370 ± 2.211		
Oropharynx	6	8.82	3.023 ± 2.471		
Local invasion					
No	42	61.76	4.659 ± 3.851	Z = 1.540	0.124
Yes	26	38.24	3.637 ± 3.903		
Tumor type					
Primary	57	83.82	4.252 ± 4.016	Z = 0.724	0.469
Recurrent	11	16.18	4.352 ± 3.201		

Note: pN, pathological lymph node status.

[a]△Ct indicates the difference in the cycle number at which a sample's fluorescent signal passes a given threshold above the baseline (Ct) derived from the lnc-H2AFV-1 gene compared with that of β-actin in tumor tissue samples.

*$P < 0.05$.

and FISH assays (Figure 3B). The results showed that *lnc-H2AFV-1* was predominantly localized to the nucleus.

3.4 | *Lnc-H2AFV-1* promoted tumor growth in nude mice models

Tumor volumes were significantly larger and tumors were significantly heavier in mice subcutaneously injected with HN6 cells stably transduced with LV-lnc-H2AFV-1 compared to the LV-NC group (Figure 4A). The H&E and Ki-67 staining results further confirmed changes in tumor formation (Figure 4B). In addition, qPCR showed that the three ASOs silenced *lnc-H2AFV-1* expression in CAL-27 cells, and then cholesterol-conjugated ASO-2 (ASO-lnc-H2AFV-1) and ASO-NC from RiboBio were used for in vivo ASO delivery in xenograft nude mice (Figure 4C). The volume and weight of xenografts were significantly decreased in mice treated with ASO-lnc-H2AFV-1 compared to ASO-NC group (Figure 4D). Staining with H&E and Ki-67 revealed pathological changes in the ASO-treated xenografts (Figure 4E). The results showed that *lnc-H2AFV-1* promoted HNSCC cell growth in vivo.

3.5 | *Lnc-H2AFV-1* increased m6A modification in head and neck squamous cell carcinoma cells

To determine whether m6A modification was regulated by *lnc-H2AFV-1*, we measured global m6A levels in HNSCC cells with *lnc-H2AFV-1* knockdown or overexpression by quantifying m6A dot blots and RNA methylation. Levels of m6A were substantially decreased by *lnc-H2AFV-1* knockdown in CAL27 and SCC-9 cells, whereas m6A levels were substantially increased with the overexpression of *lnc-H2AFV-1* in HN6 and SCC-9 cells (Figure 5A–C). Furthermore, western blotting showed that *lnc-H2AFV-1* knockdown significantly decreased METTL3/14 levels but increased FTO expression in CAL-27 and SCC-9 cells, whereas *lnc-H2AFV-1* overexpression significantly increased METTL3/14 levels but decreased FTO expression in HN6 and SCC-9 cells, (Figure 5D,

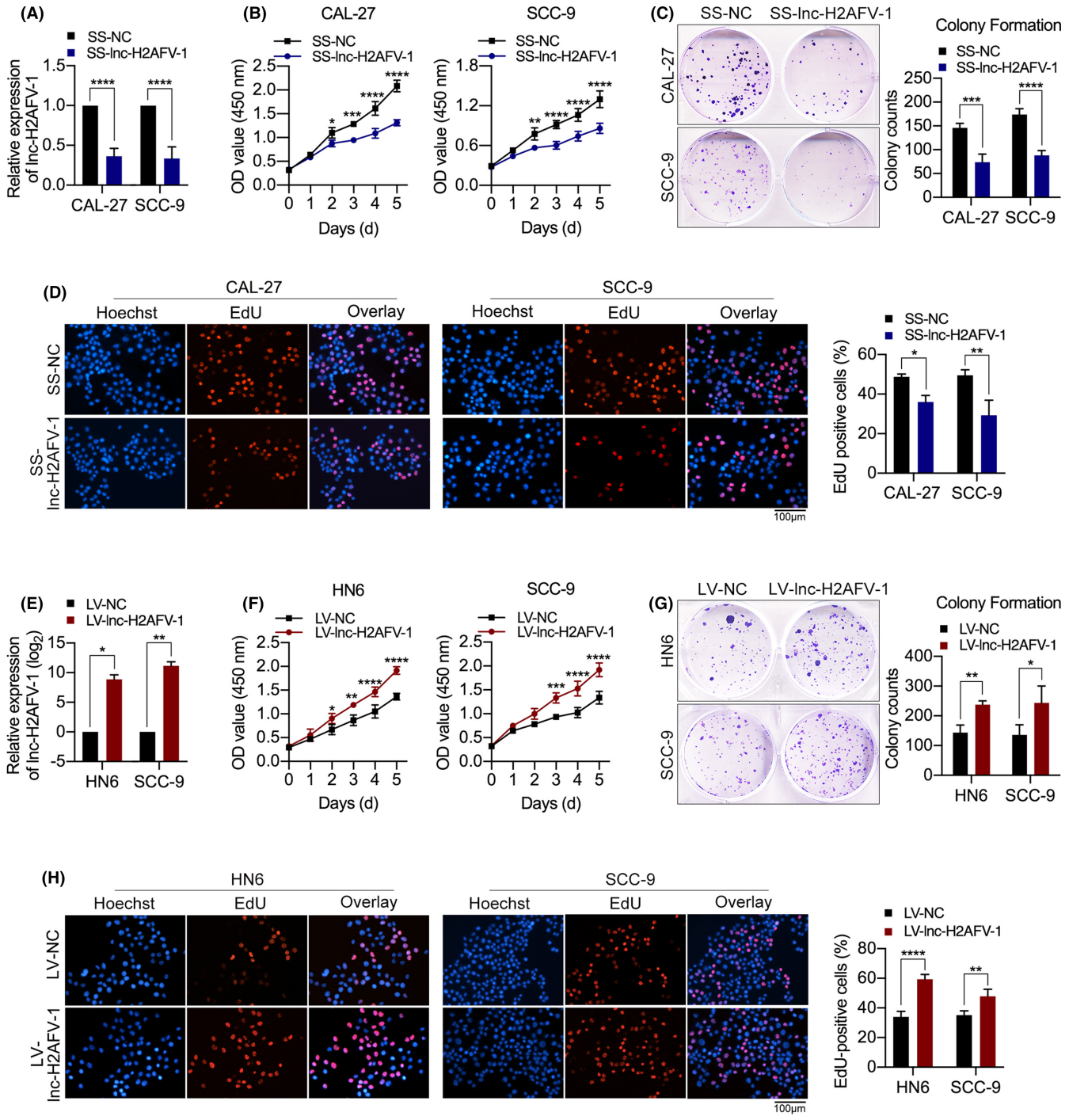

FIGURE 2 Effects of *lnc-H2AFV-1* on head and neck squamous cell carcinoma (HNSCC) cell proliferation in vitro. (A) Relative expression of *lnc-H2AFV-1* in CAL-27 and SCC-9 cells transfected with *lnc-H2AFV-1* smart silencer (SS-lnc-H2AFV-1) at 24 h determined by quantitative real-time PCR (qPCR). (B) Effects of *lnc-H2AFV-1* expression on proliferation of CAL-27 and SCC-9 cells transfected with SS-lnc-H2AFV-1 determined using CCK-8 assays. (C) Abilities of CAL-27 and SCC-9 cells transfected with SS-lnc-H2AFV-1 to form colonies, as determined by colony formation assays. (D) Proliferation abilities of CAL-27 and SCC-9 cells transfected with SS-lnc-H2AFV-1, as detected using EdU assays. (E) Relative expression of *lnc-H2AFV-1* in HN6 and SCC-9 cells stably transduced with *lnc-H2AFV-1* vector (LV-lnc-H2AFV-1), as detected by qPCR. (F) Effects of *lnc-H2AFV-1* expression on cell proliferation evaluated by CCK-8 assays in HN6 and SCC-9 cells stably transduced with LV-lnc-H2AFV-1. (G) Colonizing abilities of HN6 and SCC-9 cells stably transduced with LV-lnc-H2AFV-1, as determined by colony formation assays. (H) Proliferation of HN6 and SCC-9 cells stably transduced with LV-lnc-H2AFV-1, as detected using EdU assays. Scale bar: 100 μm. $^{*}P < 0.05$, $^{**}P < 0.01$, $^{***}P < 0.001$, $^{****}P < 0.0001$

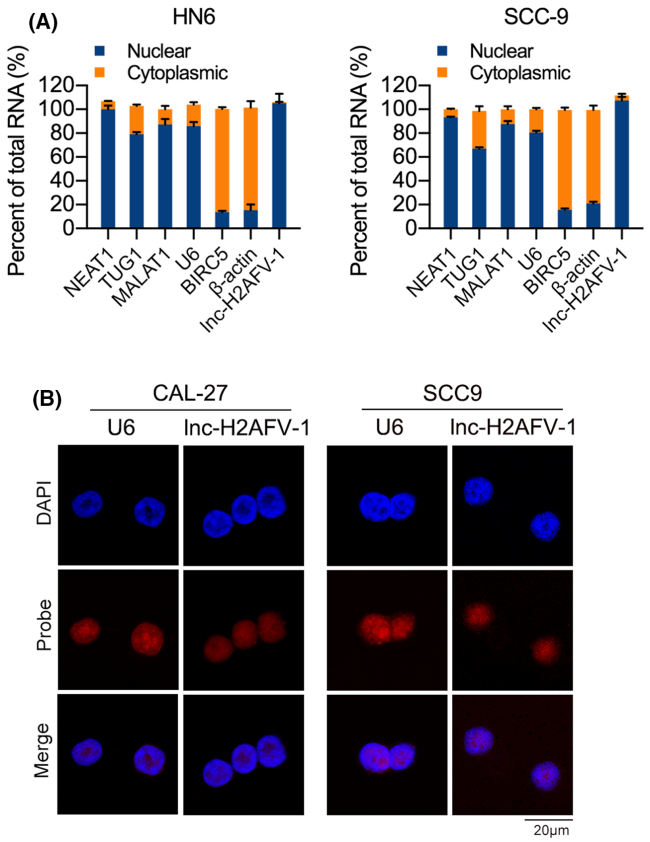

FIGURE 3 Subcellular distribution of *lnc-H2AFV-1* in head and neck squamous cell carcinoma (HNSCC) cells. (A) Cell nucleus/cytoplasm fractionation shows distribution of *lnc-H2AFV-1* in HN6 and SCC-9 cells. *NEAT1*, *TUG1*, *MALAT1*, *U6*, *BIRC5*, and β-actin served as endogenous controls. (B) FISH analysis of *lnc-H2AFV-1* in CAL-27 and SCC-9 cells. Scale bar: 20 μm

E). These results showed that *lnc-H2AFV-1* modulated global m6A methylation levels by regulating the methyltransferases METTL3/14 and the demethylase FTO.

3.6 | Intraflagellar transport 80 is a downstream m6A modified target of *lnc-H2AFV-1*

We elucidated the mechanisms underlying the effects of *lnc-H2AFV-1* on m6A methylation by MeRIP-seq analysis of HN6 cells stably overexpressing *lnc-H2AFV-1* (LV-lnc-H2AFV-1 group) and the LV-NC group. The MeRIP-sequencing data have been deposited in the NCBI GEO database: GSE196769. Metagene analysis showed that the m6A peaks in two groups were both predominantly enriched near the stop codon. However, m6A peaks in the LV-lnc-H2AFV-1 group showed a distinct pattern from peaks in the LV-NC group in the 5′UTR (Figure 6A). The distribution proportion of m6A peaks in 5′UTR and 3′UTR in the LV-lnc-H2AFV-1 group was larger than that in the LV-NC group (Figure 6B). The AAAC motif was highly enriched within m6A sites (Figure 6C). Compared with the LV-NC group, the LV-lnc-H2AFV-1 group had 1627 significantly upregulated m6A peaks corresponding to transcripts of 1432 genes, and 812 significantly downregulated m6A peaks representing transcripts of 767 genes (Figure 6D,E). The distribution proportion of differential m6A peaks (LV-lnc-H2AFV-1 *vs* LV-NC) in the 5′UTRs is 20.09%, and that in 3′UTRs is 38.79% (Figure 6F). In addition, the LV-lnc-H2AFV-1 group had 518 significantly upregulated genes and 60 significantly downregulated genes compared with the LV-NC group (Figure 6G,H). We further identified 175 hypermethylated m6A genes whose mRNA transcripts were upregulated (Hyper-up) in the LV-lnc-H2AFV-1 group, compared with the LV-NC group (Figure 6I). Gene Ontology (GO) analysis revealed abundant hyper-up genes in the regulation of cell division, transcription, protein deubiquitination, and other terms (Figure S3A). Moreover, pathway analysis demonstrated that the hyper-up genes are mainly involved in various cancer-related pathways (Figure S3B). We placed more emphasis on the hyper-up genes with differential m6A peaks distributing in the 5′UTR or 3′UTR and found 90 shared genes (Figure 6J). The top 10 genes with the most enriched m6A peaks and the highest expression are listed in Table S4. We further verified the mRNA expression of these 10 genes in *lnc-H2AFV-1*-overexpressed HN6 and SCC-9 cells and found that the mRNA expression of *IFT80* and caspase 8-associated protein 2 (*CASP8AP2*) was upregulated, consistent with *lnc-H2AFV-1* expression (Figure 6K and Figure S3C,D). In addition, the expression of *IFT80* was downregulated with the decrease of *lnc-H2AFV-1* expression (Figure 6L). Further MeRIP-qPCR assays showed that *IFT80* m6A modifications were significantly upregulated due to *lnc-H2AFV-1* overexpression, but *CASP8AP2* had no similar results (Figure 6M, Figure S3E). The m6A peak of *IFT80* induced by *lnc-H2AFV-1* overexpression was visualized using IGV (Figure 6N). From the above, *IFT80* was identified as a downstream m6A modified target of *lnc-H2AFV-1*.

3.7 | *IFT80* mediated the function of *lnc-H2AFV-1* to promote head and neck squamous cell carcinoma cell proliferation

We evaluated the expression of *IFT80* mRNA in HNSCC from the Tumor Immune Estimation Resource (TIMER; http://timer.cistrome.org)[29], GEPIA, ENCORI, and UALCAN (http://ualcan.path.uab.edu)[30] databases. The database results showed that *IFT80* is generally upregulated in HNSCC tissues compared to normal tissues (Figure S4A–D). Moreover, the expression of *IFT80* was associated with tumor grade and lymph node metastasis (Figure S4E,F). Similarly, our results showed that *IFT80* mRNA expression was significantly upregulated in 68 HNSCC tissues compared to their adjacent normal tissues (Figure 7A,B) and positively associated with *lnc-H2AFV-1* expression in HNSCC tissues (Figure 7C).

In addition, *IFT80* expression was upregulated in most HNSCC cell lines (Figure 7D). CAL-27 cells were, respectively, transfected

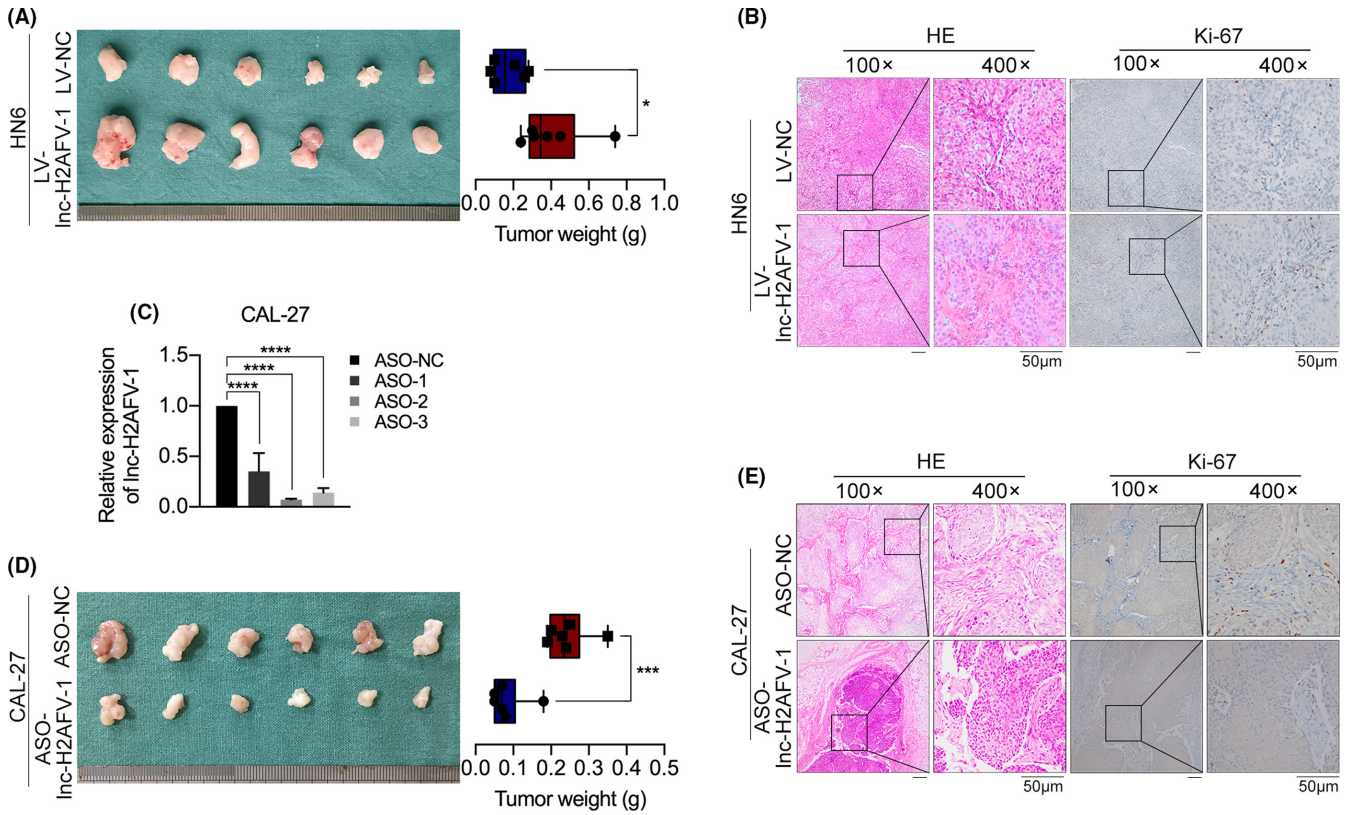

FIGURE 4 *Lnc-H2AFV-1* promotes head and neck squamous cell carcinoma (HNSCC) cell growth in vivo. (A) Tumor volume and weight in nude mice subcutaneously inoculated with HN6 cells stably transduced with *lnc-H2AFV-1* at end of experiment. $n = 6$/group. (B) H&E staining and immunohistochemistry (IHC) of Ki-67 in xenograft tissues. Scale bar: 50 μm. (C) Silencing efficiency of ASO-1, ASO-2, and ASO-3 included in SS-lnc-H2AFV-1 in CAL-27 cells, as determined by quantitative real-time PCR (qPCR). (D) Volumes and weights of tumors from CAL-27 tumor-bearing nude mice given cholesterol-conjugated ASO-lnc-H2AFV-1 or ASO-NC. $n = 6$/group. (E) H&E staining and IHC of Ki-67 in xenograft tissues. Scale bar: 50 μm. $^{*}P < 0.05$, $^{***}P < 0.001$, $^{****}P < 0.0001$

with three siRNAs (si-1, si-2, si-3) targeting *IFT80* to knock down the relative expression of *IFT80*, and si-3 (si-IFT80) was selected for subsequent experiments (Figure S5A). *IFT80* knockdown significantly suppressed CAL-27 cell proliferation according to the findings of CCK-8, colony formation, and EdU assays (Figure S5B–D). Furthermore, *IFT80* was overexpressed in HN6 cells through transfection with *IFT80* vector (Figure S5E). *IFT80* overexpression promoted cell proliferation according to the findings of CCK-8, colony formation, and EdU assays (Figure S5F–H). Further, the results of rescue experiments showed that the increased cell growth due to *lnc-H2AFV-1* overexpression could be restored again when *IFT80* was knocked down in HN6 cells, and the cell growth inhibition due to *lnc-H2AFV-1* knockdown could be restored when *IFT80* was overexpressed in CAL-27 cells (Figure 7E–J).

The relative mRNA expression of *IFT80* significantly decreased after METTL3 or METTL14 knockdown in CAL-27 cells (Figure S5I). Moreover, METTL3 or METTL14 knockdown reversed *IFT80* expression in *lnc-H2AFV-1*-overexpressing HN6 cells (Figure S5J). We concluded that *lnc-H2AFV-1* promoted m6A modification by regulating METTL3/14 and FTO, thereby regulating the expression and m6A modification level of IFT80, leading to HNSCC proliferation (Figure 7K).

4 | DISCUSSION

The initiation and development of HNSCC is a multistep process involving the gradual acquisition of genetic and epigenetic alterations that lead to the uncontrolled growth and proliferation of tumor cells. Therefore, elucidating the underlying molecular events that account for HNSCC tumorigenesis is important.[14] Many upregulated lncRNAs, such as LINC00460, MIR31HG, UCA1, and CASC9, promoted HNSCC progression in vivo and in vitro[8,31–33] through complex molecular mechanisms and should be effective molecular markers for cancer diagnosis and prognosis. We found that *lnc-H2AFV-1* was upregulated in HNSCC tissues and cell lines, and its overexpression was significantly associated with tumor size in patients with HNSCC. Functional analyses revealed that *lnc-H2AFV-1* knockdown significantly inhibited HNSCC cell growth in vitro and in vivo, and the results were reversed when *lnc-H2AFV-1* was overexpressed. Thus, we

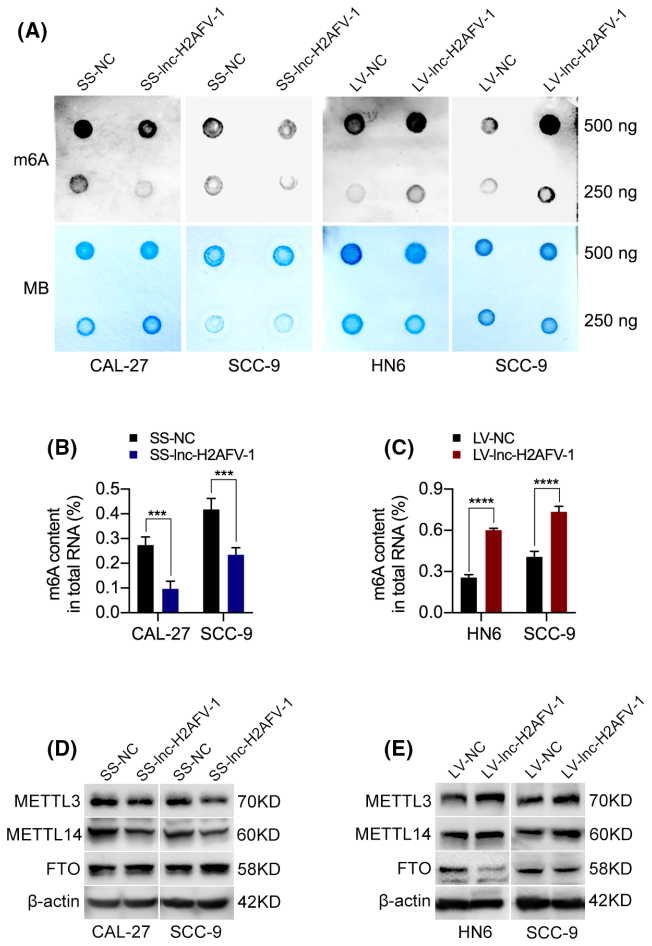

FIGURE 5 *Lnc-H2AFV-1* promotes m6A modification of head and neck squamous cell carcinoma (HNSCC) cells. (A) Levels of m6A in total RNA from HNSCC cells with *lnc-H2AFV-1* knockdown and overexpression, as determined by m6A dot blotting. Corresponding RNAs were loaded equally by twofold serial dilution to 500 and 250 ng. Methylene blue staining served as a loading control. (B, C) Content of m6A in HNSCC cells with *lnc-H2AFV-1* knockdown (B) and overexpression (C) assessed by RNA methylation quantification assays. (D, E) Western blots of METTL3, METTL14, and fat mass and obesity-associated (FTO) expression in HNSCC cells with *lnc-H2AFV-1* knockdown (D) or overexpression (E). ***$P < 0.001$, ****$P < 0.0001$

revealed that dysregulated *lnc-H2AFV-1* was closely associated with HNSCC progression.

Consistent with previous findings, m6A is the most abundant internal modification of mRNAs and lncRNAs in most eukaryotes.[34] The role of m6A is achieved through the dynamic interaction of "writers" (methyltransferases), "erasers" (demethylases), and "readers" (effector proteins).[35] The m6A modification and its regulation have dual characteristics in leukemia, lung cancer, and other tumors.[36] However, whether m6A modification is regulated by lncRNAs involved in the tumorigenesis and progression of HNSCC has remained unclear. Interactions with m6A regulators facilitate the molecular functions of lncRNAs. For instance, lncRNA *LINRIS* interacted with IGF2BP2 and maintained IGF2BP2 expression, and the *LINRIS*-IGF2BP2-MYC axis correlated with the development of colorectal cancer.[37] Similarly, *LNC942* directly recruited METTL14 protein by harboring a specific recognition sequence and promoted cell proliferation and growth in breast cancer.[38] The present study revealed that *lnc-H2AFV-1* could significantly upregulate the global m6A level of HNSCC cells, highlighting the important function of *lnc-H2AFV-1* in m6A modification. Furthermore, *lnc-H2AFV-1* influenced m6A modification by regulating METTL3/14 and FTO expression. Our MeRIP-seq data results showed that m6A peaks in HN6 cells were enriched near the stop codon, which was consistent with the published m6A characteristics in human transcripts.[39,40] Meanwhile, the results showed that the frequency of m6A peaks in the 5′UTR and 3′UTR is higher in the LV-lnc-H2AFV-1 group compared to the control group, so some enriched m6A peaks in the 5′UTR and 3′UTR might relate to *lnc-H2AFV-1*. Then, a subset of important oncogenes with upregulated mRNA expression and hyper-m6A modification in the 5′UTR or 3′UTR due to *lnc-H2AFV-1* overexpression was focused on. Verified by MeRIP and qPCR, the m6A modification level and mRNA expression of *IFT80* were increased in *lnc-H2AFV-1*-overexpressed HNSCC cells, and *IFT80* is the target gene for subsequent study.

IFT80 is a component of intraflagellar transport (IFT) complex B, which is indispensable for cilia formation and function.[41] Previous studies have indicated that IFT80 is overexpressed in gastric cancer and increases cell proliferation and invasion but inhibits apoptosis.[42]

FIGURE 6 Characterization of m6A modification and identification of *lnc-H2AFV-1* downstream target. (A) Distribution of m6A peaks region along all transcripts in LV-NC and LV-lnc-H2AFV-1 groups. (B) Pie chart showing m6A peak distribution in all transcripts of LV-NC and LV-lnc-H2AFV-1 groups. (C) Consensus sequence motif identified from MeRIP-seq peaks in LV-NC and LV-lnc-H2AFV-1 groups. (D) Volcano plot of differential m6A peaks. (E) Statistic of differential m6A peaks between LV-NC and LV-lnc-H2AFV-1 groups. (F) Pie chart showing the differential m6A peaks distribution in mRNA transcripts between LV-NC and LV-lnc-H2AFV-1 groups in all transcripts. (G) Volcano plot showing the differentially expressed genes between LV-NC and LV-lnc-H2AFV-1 groups. (H) Statistic of differential expressed genes between LV-NC and LV-lnc-H2AFV-1 groups. (I) Distribution of genes with significant changes in both m6A level ($\log_2$ FC) and RNA expression level ($\log_2$ FC) in LV-NC and LV-lnc-H2AFV-1 groups. (J) Venn diagram showing the hyper-up genes with differential m6A peaks distributing in 5′UTR or 3′UTR. The top 10 hypermethylated m6A and differentially up-expressed genes are shown. (K) Relative expression of *IFT80* in HN6 and SCC-9 cells stably transduced with LV-lnc-H2AFV-1 or LV-NC by quantitative real-time PCR (qPCR). (L) Relative expression of *IFT80* in CAL-27 and SCC-9 cells transfected with SS-lnc-H2AFV-1 or SS-NC by qPCR. (M) m6A level of *IFT80* quantified by MeRIP-qPCR in LV-lnc-H2AFV-1 and LV-NC group. (N) The m6A modification site of *IFT80* mRNA determined using the Integrated Genomics Viewer. *$P < 0.05$, **$P < 0.01$, ****$P < 0.0001$; ns, no significance

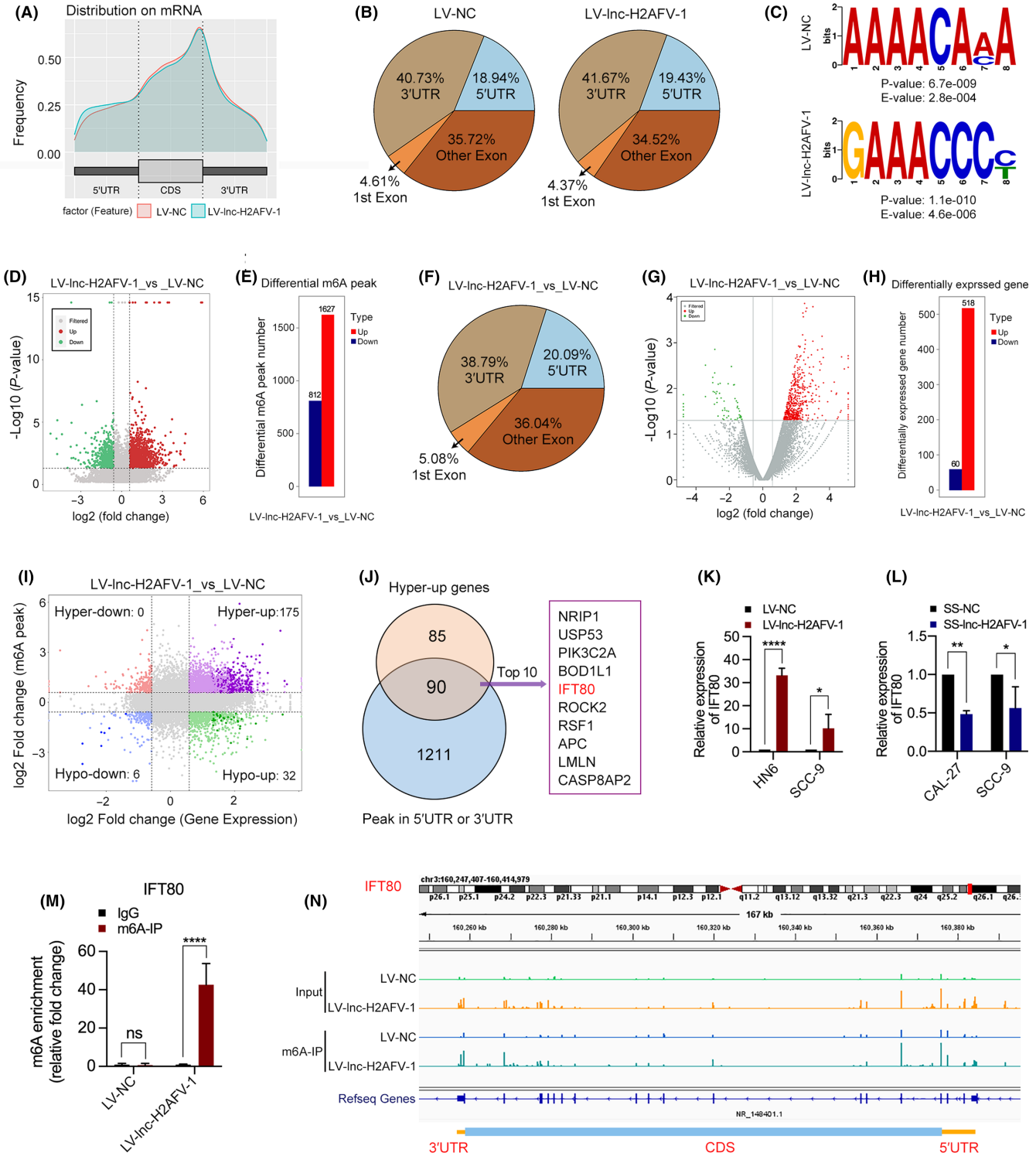

The present results from TCGA databases and collected HNSCC tissue samples have suggested that *IFT80* is upregulated in HNSCC tissues and might play a vital role in HNSCC progression. The present study showed that *IFT80* expression was positively correlated with *lnc-H2AFV-1* expression, and *IFT80* could promote HNSCC cell proliferation. It also showed that the expression and function of *lnc-H2AFV-1* and *IFT80* are consistent. *IFT80* expression was significantly decreased after METTL3 or METTL14 knockdown, and METTL3/14 knockdown reversed *IFT80* expression in *lnc-H2AFV-1*-overexpressing HNSCC cells.

These findings indicated that *lnc-H2AFV-1* affected m6A modification in HNSCC cells by regulating METTL3/14 and FTO and then modulated the m6A modification level of its downstream target *IFT80*. Therefore, *lnc-H2AFV-1* might serve as a potential biomarker

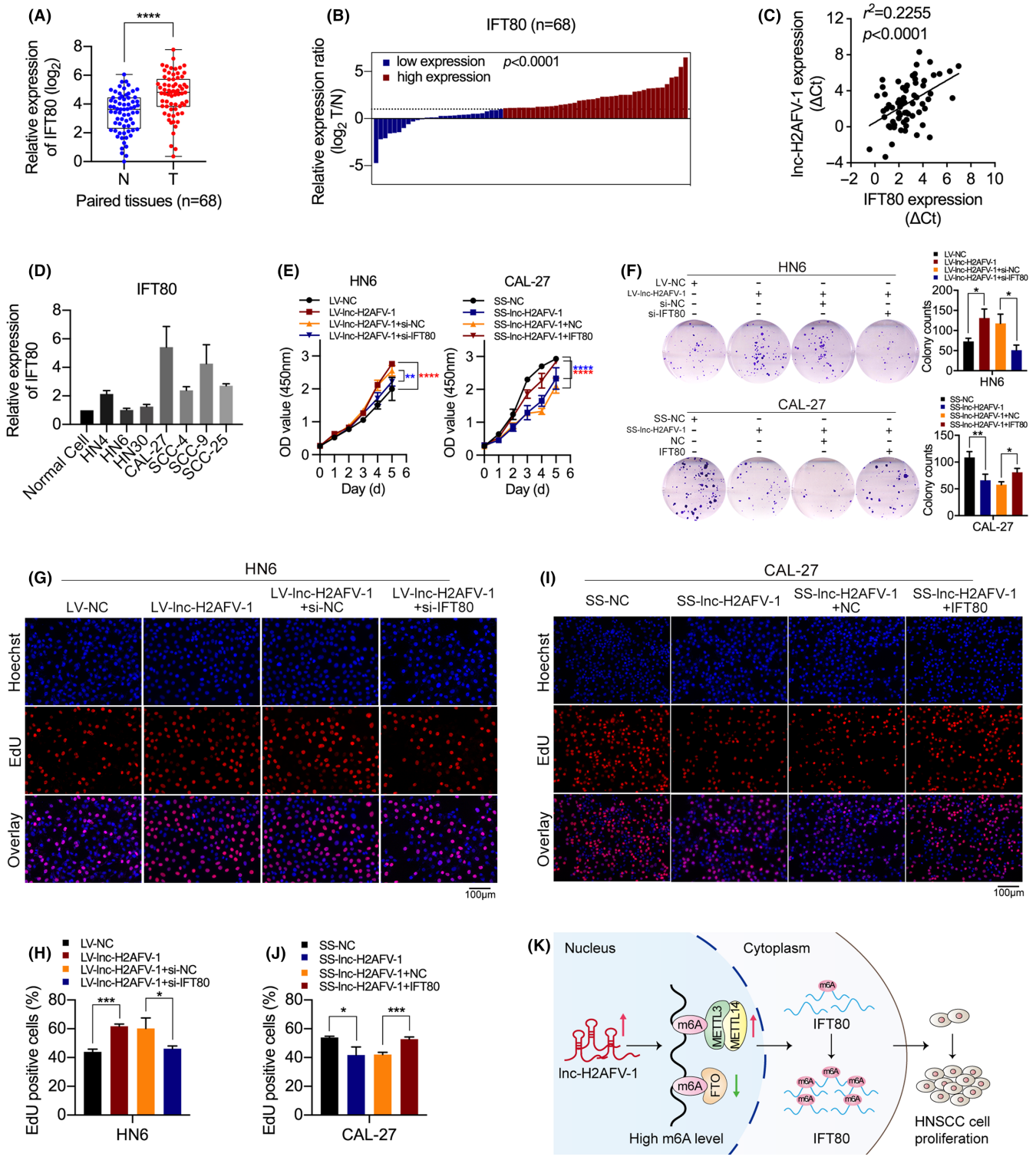

FIGURE 7 *IFT80* mediated the function of *lnc-H2AFV-1* to promote head and neck squamous cell carcinoma (HNSCC) cell proliferation. (A) Relative expression of *IFT80* in HNSCC (T) and adjacent normal (N) tissues determined using quantitative real-time PCR (qPCR) ($n = 68$). (B) Classification of *IFT80* expression into groups according to expression ratios of HNSCC tumors to adjacent normal (T/N) tissues ($n = 68$, $p < 0.0001$). (C) Pearson correlation analysis of *lnc-H2AFV-1* and *IFT80* expression in HNSCC tissue ($r^2 = 0.2255$, $n = 68$, $p < 0.0001$). (D) Relative expression of *IFT80* in seven HNSCC cell lines and normal oral epithelial cells, detected using qPCR. (E) Cell proliferation determined by CCK-8 assays when *IFT80* was knocked down in HN6 cells stably transduced with LV-lnc-H2AFV-1 or *IFT80* was overexpressed in CAL-27 cells transfected with SS-lnc-H2AFV-1. (F) Colony formation abilities determined by colony formation assays when *IFT80* was knocked down in HN6 cells stably transduced with LV-lnc-H2AFV-1 or *IFT80* was overexpressed in CAL-27 cells transfected with SS-lnc-H2AFV-1. (G, H) Effects of *IFT80* knockdown on cell proliferation of HN6 cells stably transduced with LV-lnc-H2AFV-1, as detected using EdU assays. (I, J) Effects of *IFT80* overexpression on cell proliferation of CAL-27 cells transfected with SS-lnc-H2AFV-1, as detected using EdU assays. (K) Proposed model shows modulatory role of *lnc-H2AFV-1* and m6A modifications in regulating HNSCC cell proliferation. $^*P < 0.05$, $^{**}P < 0.01$, $^{***}P < 0.001$, $^{****}P < 0.0001$

and play an important role in promoting HNSCC cell proliferation by regulating aberrant m6A RNA methylation.

ACKNOWLEDGMENTS

The authors would like to thank the "Sharing platform for the tissue sample and bioinformatics database of oral maxillofacial tumors" (Shanghai, China) and Dr Mingyu Li for their assistance. We also wish to thank Dr Qidong Zu (OE Biotech, Shanghai, China, https://www.oebiotech.com/) for assistance with the bioinformatic analyses of the MeRIP-sequencing data.

DISCLOSURE

The authors have no conflicts of interest to declare

ORCID

Yingying Jiang https://orcid.org/0000-0001-9671-7548

REFERENCES

1. Chen W, Zheng R, Baade PD, et al. Cancer statistics in China, 2015. *CA Cancer J Clin*. 2016;66:115-132.
2. Chow LQM. Head and neck cancer. *N Engl J Med*. 2020;382:60-72.
3. Siegel RL, Miller KD, Fuchs HE, Jemal A. Cancer statistics, 2022. *CA Cancer J Clin*. 2022;72:7-33.
4. Hedberg ML, Goh G, Chiosea SI, et al. Genetic landscape of metastatic and recurrent head and neck squamous cell carcinoma. *J Clin Invest*. 2016;126:169-180.
5. Lee JT. Epigenetic regulation by long noncoding RNAs. *Science*. 2012;338:1435-1439.
6. Dhamija S, Diederichs S. From junk to master regulators of invasion: lncRNA functions in migration, EMT and metastasis. *Int J Cancer*. 2016;139:269-280.
7. Jiang Y, Wu K, Cao W, et al. Long noncoding RNA KTN1-AS1 promotes head and neck squamous cell carcinoma cell epithelial–mesenchymal transition by targeting miR-153-3p. *Epigenomics*. 2020;12:487-505.
8. Jiang Y, Cao W, Wu K, et al. LncRNA LINC00460 promotes EMT in head and neck squamous cell carcinoma by facilitating peroxiredoxin-1 into the nucleus. *J Exp Clin Cancer Res*. 2019;38:365.
9. Desrosiers R, Friderici K, Rottman F. Identification of methylated nucleosides in messenger RNA from Novikoff hepatoma cells. *Proc Natl Acad Sci USA*. 1974;71:3971-3975.
10. Li Z, Weng H, Su R, et al. FTO plays an oncogenic role in acute myeloid leukemia as a N(6)-methyladenosine RNA demethylase. *Cancer Cell*. 2017;31:127-141.
11. Cai X, Wang X, Cao C, et al. HBXIP-elevated methyltransferase METTL3 promotes the progression of breast cancer via inhibiting tumor suppressor let-7g. *Cancer Lett*. 2018;415:11-19.
12. Chen X, Xu MU, Xu X, et al. METTL14-mediated N6-methyladenosine modification of SOX4 mRNA inhibits tumor metastasis in colorectal cancer. *Mol Cancer*. 2020;19:106.
13. Chen Y, Peng C, Chen J, et al. WTAP facilitates progression of hepatocellular carcinoma via m6A-HuR-dependent epigenetic silencing of ETS1. *Mol Cancer*. 2019;18:127.
14. Zhao X, Cui L. Development and validation of a m(6)A RNA methylation regulators-based signature for predicting the prognosis of head and neck squamous cell carcinoma. *Am J Cancer Res*. 2019;9:2156-2169.
15. Yi L, Wu G, Guo L, Zou X, Huang P. Comprehensive analysis of the PD-L1 and immune infiltrates of m(6)A RNA methylation regulators in head and neck squamous cell carcinoma. *Mol Ther Nucleic Acids*. 2020;21:299-314.
16. Liu L, Lei X, Fang Z, Tang Y, Meng J, Wei Z. LITHOPHONE: improving lncRNA methylation site prediction using an ensemble predictor. *Front Genet*. 2020;11:545.
17. Zhang Z, Yang J, Feng Q, et al. Compositional and functional analysis of the microbiome in tissue and saliva of oral squamous cell carcinoma. *Front Microbiol*. 2019;10:1439.
18. Jiang Y, Guo H, Tong T, et al. lncRNA lnc-POP1-1 upregulated by VN1R5 promotes cisplatin resistance in head and neck squamous cell carcinoma through interaction with MCM5. *Mol Ther*. 2022;30:448-467.
19. Zeng Y, Wang S, Gao S, et al. Refined RIP-seq protocol for epitranscriptome analysis with low input materials. *PLoS Biol*. 2018;16:e2006092.
20. Kim D, Langmead B, Salzberg SL. HISAT: a fast spliced aligner with low memory requirements. *Nat Methods*. 2015;12:357-360.
21. Cui X, Zhang L, Meng J, Rao MK, Chen Y, Huang Y. MeTDiff: a novel differential RNA methylation analysis for MeRIP-Seq data. *IEEE/ACM Trans Comput Biol Bioinform*. 2018;15:526-534.
22. Bailey TL, Boden M, Buske FA, et al. MEME SUITE: tools for motif discovery and searching. *Nucleic Acids Res*. 2009;37(Web Server):W202-W208.
23. Robinson JT, Thorvaldsdóttir H, Wenger AM, Zehir A, Mesirov JP. Variant review with the integrative genomics viewer. *Cancer Res*. 2017;77:e31-e34.
24. Volders P-J, Anckaert J, Verheggen K, et al. LNCipedia 5: towards a reference set of human long non-coding RNAs. *Nucleic Acids Res*. 2019;47:D135-D139.
25. Howe KL, Achuthan P, Allen J, et al. Ensembl 2021. *Nucleic Acids Res*. 2021;49:D884-D891.
26. Li JH, Liu S, Zhou H, Qu LH, Yang JH. starBase v2.0: decoding miRNA-ceRNA, miRNA-ncRNA and protein–RNA interaction networks from large-scale CLIP-Seq data. *Nucleic Acids Res*. 2014;42:D92-D97.
27. Tang Z, Li C, Kang B, Gao G, Li C, Zhang Z. GEPIA: a web server for cancer and normal gene expression profiling and interactive analyses. *Nucleic Acids Res*. 2017;45:W98-W102.
28. Bao Z, Yang Z, Huang Z, Zhou Y, Cui Q, Dong D. LncRNADisease 2.0: an updated database of long non-coding RNA-associated diseases. *Nucleic Acids Res*. 2019;47:D1034-D1037.
29. Li T, Fu J, Zeng Z, et al. TIMER2.0 for analysis of tumor-infiltrating immune cells. *Nucleic Acids Res*. 2020;48:W509-W514.
30. Chandrashekar DS, Bashel B, Balasubramanya SAH, et al. UALCAN: a portal for facilitating tumor subgroup gene expression and survival analyses. *Neoplasia*. 2017;19:649-658.
31. Wang RU, Ma Z, Feng L, et al. LncRNA MIR31HG targets HIF1A and P21 to facilitate head and neck cancer cell proliferation and tumorigenesis by promoting cell-cycle progression. *Mol Cancer*. 2018;17:162.
32. Fang Z, Zhao J, Xie W, Sun Q, Wang H, Qiao B. LncRNA UCA1 promotes proliferation and cisplatin resistance of oral squamous cell carcinoma by sunppressing miR-184 expression. *Cancer Med*. 2017;6:2897-2908.
33. Yang Y, Chen D, Liu H, Yang K. Increased expression of lncRNA CASC9 promotes tumor progression by suppressing autophagy-mediated cell apoptosis via the AKT/mTOR pathway in oral squamous cell carcinoma. *Cell Death Dis*. 2019;10:41.
34. Liu ZX, Li LM, Sun HL, Liu SM. Link Between m6A Modification and Cancers. *Front Bioeng Biotechnol*. 2018;6:89.
35. Ping X-L, Sun B-F, Wang LU, et al. Mammalian WTAP is a regulatory subunit of the RNA N6-methyladenosine methyltransferase. *Cell Res*. 2014;24:177-189.
36. Ma S, Chen C, Ji X, et al. The interplay between m6A RNA methylation and noncoding RNA in cancer. *J Hematol Oncol*. 2019;12:121.
37. Wang Y, Lu J-H, Wu Q-N, et al. LncRNA LINRIS stabilizes IGF2BP2 and promotes the aerobic glycolysis in colorectal cancer. *Mol Cancer*. 2019;18:174.

38. Sun T, Wu Z, Wang X, et al. LNC942 promoting METTL14-mediated m(6)A methylation in breast cancer cell proliferation and progression. *Oncogene*. 2020;39:5358-5372.
39. Meyer KD, Saletore Y, Zumbo P, Elemento O, Mason CE, Jaffrey SR. Comprehensive analysis of mRNA methylation reveals enrichment in 3′UTRs and near stop codons. *Cell*. 2012;149:1635-1646.
40. Liu L, Wu YU, Li Q, et al. METTL3 promotes tumorigenesis and metastasis through BMI1 m(6)A methylation in oral squamous cell carcinoma. *Mol Ther*. 2020;28:2177-2190.
41. Yuan X, Cao J, He X, et al. Ciliary IFT80 balances canonical versus non-canonical hedgehog signalling for osteoblast differentiation. *Nat Commun*. 2016;7:11024.
42. Wang R, Deng X, Yuan C, et al. IFT80 improves invasion ability in gastric cancer cell line via ift80/p75NGFR/MMP9 signaling. *Int J Mol Sci*. 2018;19:3616.

SUPPORTING INFORMATION

Additional supporting information may be found in the online version of the article at the publisher's website.

How to cite this article: Chen X, Liu Y, Sun D, et al. Long noncoding RNA *lnc-H2AFV-1* promotes cell growth by regulating aberrant m6A RNA modification in head and neck squamous cell carcinoma. *Cancer Sci*. 2022;113:2071–2084. doi:10.1111/cas.15366